Phonon renormalization and c-axis phonon-plasmon mixing in La_2CuO_4

Claus Falter, Michael Klenner, and Georg A. Hoffmann
Institut für Theoretische Physik II - Festkörperphysik, Universität Münster, Wilhelm-Klemm-Strasse 10, 48149 Münster, Germany
(Received 7 February 1995)

A decomposition of the electronic-density response recently worked out for the description of local, nonlocal, and nonadiabatic electron-phonon interaction effects in the high-temperature superconductors is applied to the lattice dynamics and phonon-plasmon mixing in La_2CuO_4. The local part of the density response and the electron-phonon interaction is approximated by an improved model of rigid ions using effective ionic charges as calculated from a tight-binding analysis of the first-principles electronic band structure. Moreover, covalence effects are simulated by scaling the short-range part of the relevant *ab initio* pair potentials. Such a model serves as a reference system describing the insulating phase. Phonon dispersion curves are calculated in this model and good overall agreement with recent experiments is found. In the case of the metallic phase, specific nonlocal screening effects in terms of localized charge fluctuations are additionally introduced at the ions by a parameter-free procedure. In the framework of the improved reference system, phonon dispersion curves and phonon-induced changes of the crystal potential are calculated for the metallic phase. Characteristic changes in the phonon dispersion produced by the insulator-metal transition are discussed and compared with the experiments. Further, c-axis phonon-plasmon mixing is investigated. Phonon-plasmon coupling leads in particular to an additional softening of the symmetrical apical oxygen breathing mode at the Z point (O_Z^z) being important in context with nonlocal electron-phonon interaction and pair binding. In this way the already large decrease in frequency of this phonon predicted in our earlier work in the adiabatic approximation as compared to the calculated frequency of O_Z^z in the insulating phase is further enhanced. The anomalous large renormalization of this mode has been confirmed quite recently by the experiments. A final remark is concerned with the oxygen isotope effect in the high-temperature superconductors from the viewpoint of phonon-plasmon coupling.

I. INTRODUCTION

On the route towards an understanding of the mechanism leading to an increased pair binding in the high-temperature superconductors (HTSC's), it is quite natural to investigate first the electron-phonon interaction (EPI) and to separate features which are normal, like local EPI effects, from those which are specific for the HTSC's. Such attempts have been undertaken, e.g., in Refs. 1–5. In particular, the calculations in Refs. 2–4 indicate that unusual strong nonlocal (long-range) EPI effects appear for certain phonon modes as a consequence of an interplay of the layered crystal structure, the quasi-two-dimensional electronic band structure, and strong ionic forces which are only weakly screened through a mechanism dominated by ionic charge fluctuations. So far most of these calculations [and of course also all frozen-phonon calculations within density-functional theory (DFT)] have been performed using the adiabatic approximation, which relies on static screening. As a consequence the important long-range Coulomb correlations which give rise to the (low-lying) plasmon modes via dynamical screening and the coupling to the phonons as discussed below are excluded. The local (rigid) part of the density response and of the EPI in our description has been approximated by a proper *ab initio* model of rigid ions.[2–4,6] Using such a model as a reference system to approximate the insulating phase of the HTSC's, nonlocal (nonrigid) contributions to the density response are additionally taken into account in the form of electronic charge fluctuations on the ions in order to generalize the model for a suitable representation of the metallic phase. Our calculations in Refs. 2–4 for La_2CuO_4 have shown that many important features of the experimental phonon dispersion can be understood within such an approach.

A certain problem with the ionic reference model in these calculations using nominal charges for the ions is the width of the phonon spectrum which apparently is overestimated, similarly as in the potential-induced breathing model.[1] In the present paper we shall improve upon this point by employing effective ionic charges instead of the nominal ones. These charges are derived from a tight-binding analysis of the electronic band structure as given in Ref. 7. A further improvement can be achieved simulating covalence effects by scaling the short-range part of the relevant pair potentials.

A nonadiabatic view of electron-phonon coupling and lattice dynamics has been suggested for high-frequency phonon modes propagating along the $\Lambda \sim (0,0,1)$ direction, i.e., along the c axis, in the HTSC's[4] and recent calculations on the basis of the ionic reference system with nominal ionic charges and without covalence corrections have shown that there should be mode mixing between these phonons and a low-energy plasmon whenever the dispersion of the electronic bands in the c direction is sufficiently small at the Fermi level.[6] The latter is very

0163-1829/95/52(5)/3702(9)/$06.00

likely to be the case.[1,5,8] The question of possible c-axis phonon-plasmon mixing, phonon renormalization, and a nonadiabatic enhancement of the phonon-induced changes of the site-potential being crucial for pairing will be investigated in this paper, applying the improved model for the description of the insulating phase of La_2CuO_4 and simultaneously as a reference model for the metallic phase.

The remaining part of the paper is organized in the following way. In Sec. II a sketch of the main aspects of the theory and the model is provided. Section III gives a comparison of the results for the phonon dispersion in the old and the improved reference models for the insulating phase as well as for the metallic phase in adiabatic approximation. The nonadiabatic enhancement of electron-phonon coupling is discussed in Sec. IV using the symmetrical apical oxygen breathing mode at the Z point (O_Z^z mode) as an important example. Further, the coupled phonon-plasmon dispersion along the c axis is calculated on the basis of the new model. Finally, consequences for the oxygen isotope effect are outlined. In Sec. V we summarize our main results and mention a possible implication of the low-energy coupled modes for the c-axis transport.

II. THEORY AND MODELING

The details of the electronic-density response description which finally yields the coupled phonon-plasmon modes can be found in Refs. 2–4, and 6. So in the following only a sketch of the main aspects of the theory is given.

The local part of the density response and the EPI, respectively, is approximated by a proper *(ab initio)* ionic model of rigid ions of Kim-Gordon type to represent the important effects of the ionic forces in the HTSC's. In this model the crystal energy E as a function of the configuration $\{\mathbf{R}\}$ of the ions is given by a sum of pair potentials $\phi_{\alpha\beta}$ and the sum of the (constant) self-energies of the rigid ions (E_0):

$$E(\{\mathbf{R}\})=E_0+\frac{1}{2}\sum_{\mathbf{b},\alpha,\beta}{}' \phi_{\alpha\beta}(|\mathbf{R}_\beta^{\mathbf{b}}-\mathbf{R}^\alpha|) \ . \tag{1}$$

$\mathbf{b}$ denotes the unit cells in the crystal, α, β are sublattice indices, and $\mathbf{R}_\beta^{\mathbf{b}}=\mathbf{R}^{\mathbf{b}}+\mathbf{R}^\beta$. The method of Gordon and Kim[9] is used to calculate the pair potentials from the ionic densities together with the Watson-sphere approximation[10] to treat the unstable oxygen anion. The ionic densities are obtained with a modified version of the Herman-Skillman program[11] including averaged self-interaction corrections.[12] In our earlier work we have assumed the nominal charges (La^{3+}, Cu^{2+}, O^{2-}) for the ions which is by no means necessary. Actually, the (partly) covalent character of the Cu-O bonding suggests applying somewhat decreased charges.[4]

In the present paper we employ effective ionic charges instead of the nominal ones which are derived from a tight-binding analysis of the electronic band structure.[7] This can be achieved by integrating the partial density of states of the μ (tight-binding) orbital,

$$Z_\mu(E)=\frac{2}{N}\sum_{n\mathbf{k}}\delta(E_n(\mathbf{k})-E)|C_{\mu n}(\mathbf{k})|^2 \tag{2}$$

up to the Fermi energy E_F in order to obtain the occupation number $Q_\mu(E_F)$ of this particular state,

$$Q_\mu(E_F)=\frac{2}{N}\sum_{n\mathbf{k}}\Theta(E_F-E_n(\mathbf{k}))|C_{\mu n}(\mathbf{k})|^2 \ . \tag{3}$$

$C_{\mu n}(\mathbf{k})$ means the μ component of the eigenvector of band n at the wave vector $\mathbf{k}$ from the first Brillouin zone. Note that $\sum_\mu Q_\mu(E_F)$ yields the number of electrons per unit cell. The effective ionic charges are immediately given by the orbital occupation numbers as calculated from Eq. (3).

The long-range Coulomb contribution of the pair potentials is separated and treated exactly using the Ewald method, while the remaining short-range part, $\tilde{\phi}(R)$, is calculated numerically on a mesh of ion distances, and is fitted by a generalized Born-Mayer-type form. As compared to our previous work we here fit the different contributions to $\tilde{\phi}(R)$ separately[3] and use, moreover, an extended functional form,

$$f(R)=\pm\exp(\alpha+\beta R+\gamma/R) \ , \tag{4}$$

for each contribution of $\tilde{\phi}$ (α, β, and γ are fit parameters).

In order to simulate to a certain degree covalence effects in the calculations, the short-range potentials $\tilde{\phi}(R)$ of the most important interactions are scaled according to the procedure proposed in Ref. 13,

$$\tilde{\phi}(R)\rightarrow\tilde{\phi}(R-R_0) \ . \tag{5}$$

The values of R_0 are determined in such a way that the interaction energy in Eq. (1) takes its minimum as close as possible to the experimental structure. From the pair potentials the dynamical matrix for the ionic reference system is set up using the Ewald method for the long-range Coulomb part of the pair potentials. Such a model is employed to represent the insulating phase of the HTSC's.

In order to generalize the model for a suitable description of the metallic phase, additional long-range, nonlocal contributions to the density response and the EPI are introduced in the form of localized electronic charge fluctuations (CF's) on the ions by a parameter-free procedure and are calculated consistently with the ionic model, making the occupation numbers of the orbitals variable and consequently the ionic charges, too. Finally, within this formulation the displacement-induced change of the electronic density, $\mathbf{P}_\alpha^{\mathbf{a}}(\mathbf{r})$, is given by

$$\mathbf{P}_\alpha^{\mathbf{a}}(\mathbf{r})=[\mathbf{P}_\alpha^{\mathbf{a}}(\mathbf{r})]_{\mathrm{RIM}}-\sum_{\mathbf{b}\kappa}\rho_\kappa(\mathbf{r}-\mathbf{R}_\kappa^{\mathbf{b}})\mathbf{X}_{\kappa\alpha}^{\mathbf{ba}} \ . \tag{6}$$

The $\mathbf{R}_\kappa^{\mathbf{b}}$ describe the localization centers the CF's are associated with, and κ numbers the different CF's in the unit cell. $[\mathbf{P}_\alpha^{\mathbf{a}}(\mathbf{r})]_{\mathrm{RIM}}$ gives the explicit change in the density related to the movement of the rigid ions. The densities $\rho_\kappa(\mathbf{r})$ (form factors) in Eq. (6) yield the shape of the change in the density associated with the CF's and are approximated in the present model by the spherically

averaged orbital densities of the Cu d and O_{xy} p shells (O_{xy} is the oxygen in the CuO plane). The decomposition of the vector field $\mathbf{P}_\alpha^a(\mathbf{r})$ into a rigid (local) part and a nonrigid (nonlocal) part has been done in the spirit of the quasi-ion concept where such a partition can be rigorously proved.[14]

The quantity $\mathbf{X}$ that expresses the self-consistent reaction of the CF's in response to an ion displacement can be represented, in compact notation, as

$$X=\Pi\varepsilon^{-1}B \quad \text{with } \varepsilon=1+\tilde{V}\Pi \ . \tag{7}$$

Here we have introduced the dielectric function ε and the quantity B which describes the interaction between the CF's and the displaced ions. $\tilde{V}$ contains the Coulomb interaction between the electrons as well as exchange-correlation contributions. $\tilde{V}$ and B can be calculated from the ionic self-energies and pair potentials by allowing for variable occupation numbers.[6] Dynamical screening enters via the polarizability $\Pi_{\kappa\kappa'}(\mathbf{q},\omega)$ of the electronic system. ω denotes the frequency of the perturbation (phonon); $\mathbf{q}$ is a wave vector of the first Brillouin zone. For the calculation of Π for La_2CuO_4 we use an eleven-band tight-binding model for the CuO plane[3,4,6] including all Cu d and O_{xy} p orbitals. Thus Π becomes an (11×11) matrix and the indices κ can be identified with the orbital indices μ. In order to introduce interlayer coupling, we extend this model by coupling the Cu d orbitals in one layer to the nearest O_{xy} p orbitals in the two adjacent layers.[6]

The free plasmon dispersion is extracted from the condition

$$\det[\varepsilon_{\kappa\kappa'}(\mathbf{q},\omega)]=0 \ , \tag{8}$$

and the coupled mode frequencies of the phonons and the plasmons must be determined self-consistently from the secular equation for the dynamical matrix which contains ω implicitly via $\mathbf{X}$ in Eq. (7). Furthermore, we calculate the phonon-induced site-potential changes $\delta V_\kappa(\mathbf{q}\sigma,\omega_\sigma(\mathbf{q}))$ being defined as the self-consistent change of the crystal potential δV_{eff} weighted with the density form factor $\rho_\kappa(\mathbf{r}-\mathbf{R}^\kappa)$ of the electronic CF localized at $\mathbf{R}^\kappa$, i.e.,

$$\delta V_\kappa(\mathbf{q}\sigma,\omega_\sigma(\mathbf{q}))=\int dV\rho_\kappa(\mathbf{r}-\mathbf{R}^\kappa)\delta V_{\text{eff}}(\mathbf{q}\sigma,\omega_\sigma(\mathbf{q}),\mathbf{r}) \ . \tag{9}$$

$\omega_\sigma(\mathbf{q})$ is the frequency of the phonon mode with wave vector $\mathbf{q}$ and polarization σ.

III. CALCULATION OF PHONONS IN THE ADIABATIC APPROXIMATION

In this section, we compare the calculated (adiabatic) phonon dispersion of La_2CuO_4 as obtained from our previous model using nominal ionic charges with the dispersion from the improved model developed in this paper for a description of the insulating phase of the HTSC's and with new experimental results.[15] Further, calculations in the adiabatic approximation are presented for the metallic phase, demonstrating the relevance of nonlocal EPI effects of charge-fluctuation type, in particular for the renormalization of the O_Z^z mode. The strong decrease in frequency of this phonon when passing from the insulating to the metallic phase, which has been predicted in our earlier calculations,[2,3] is also present in the new model and has been confirmed quite recently by the experiments.[16]

In Fig. 1 the phonon dispersion curves of our old ionic model using nominal charges (La^{3+}, Cu^{2+}, O^{2-}) for the ions are reproduced from Ref. 3. The results are given for the tetragonal phase of La_2CuO_4 and are shown for the main symmetry directions $\Delta\sim(1,0,0)$, $\Lambda\sim(0,0,1)$ and $\Sigma\sim(1,1,0)$. Figure 2 displays the corresponding results for the new ionic model with effective ionic charges. The latter are determined from a tight-binding analysis of the first-principles electronic band structure of La_2CuO_4 as given in Ref. 7. The orbital occupation numbers $Q_\mu(E_F)$ are calculated from the electronic band structure and the eigenfunctions with the help of Eq. (3), leading to the following electron configurations: Cu, $3d^{9.24}$ $4s^{0.3}$ $4p^{0.24}$; O_{xy}, $2p^{5.42}$; O_z, $2p^{5.47}$; and La, $5d^{0.72}$. The corresponding ionic charges are $Cu^{1.22+}$, $O_{xy}{}^{1.42-}$, $O_z{}^{1.47-}$, $La^{2.28+}$.

The structure parameters for the two models, denoted as Nom (nominal charges) and Eff (effective charges), are obtained by minimization of the interaction energy in Eq. (1). The calculated values are collected in Table I. Inspecting both data sets we find only small differences,

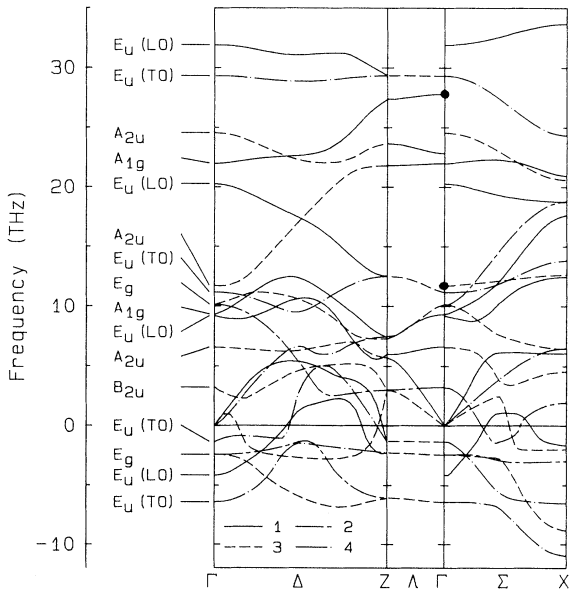

FIG. 1. Calculated phonon dispersion of the ionic reference model for La_2CuO_4 as reproduced from Ref. 3 using nominal ionic charges. The dispersion curves are shown for the main symmetry directions $\Delta\sim(1,0,0)$, $\Lambda\sim(0,0,1)$, and $\Sigma\sim(1,1,0)$. The symmetry classification of the phonon branches by irreducible representations (with labels 1–4) is realized in the figure by using different line types. Imaginary frequencies are represented as negative numbers.

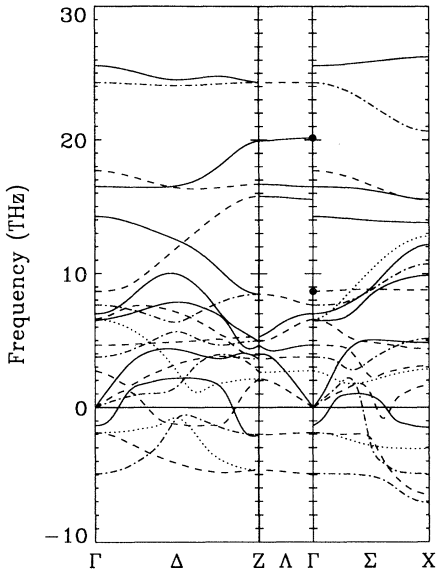

FIG. 2. Phonon dispersion of the ionic reference model for La_2CuO_4 in the main symmetry directions Δ, Λ, and Σ using effective ionic charges as calculated from a tight-binding analysis of the first-principle electronic band structure. In contrast to Fig. 1 the irreducible representation Nr. 2 is given by the line type, · · · ·.

while a comparison with the experiments shows that both models lead in particular to an enhanced planar lattice constant and to a (c/a) ratio which is too small.

Comparing the results for the phonon dispersion in Figs. 1 and 2 for the two models we realize that the main drawback of the model with nominal charges, namely, the too large width of the spectrum, which also has been found for the set of charges used in recent calculations for $YBa_2Cu_3O_6$ and $YBa_2Cu_3O_7$,[17,18] is considerably relaxed in the model with the effective charges as obtained from the tight-binding analysis of the electronic band structure. Taking the frequency of the planar oxygen breathing mode at the X point (O_X^P) (being the highest mode in both spectra) as a measure for the width we find a decrease from 33.68 to 26.24 THz. As will be seen below an approximate modeling of covalency will further decrease the frequency of O_X^P to 24.27 THz and finally, the inclusion of nonlocal screening of CF type in the metallic phase leads for O_X^P to 21.46 THz, which is in very good agreement with the experiment (21.2 THz).[15]

TABLE I. Structure parameters for La_2CuO_4 as calculated for several models (Nom, Eff, Cov 1, and Cov 2) explained in the text. For a comparison the experimental results (Ref. 20) are also given. z (O_z) and z (La) are in units of c.

La_2CuO_4	a (Å)	c/a	z (O_z)	z (La)
Nom	3.98	3.02	0.190	0.137
Eff	4.10	3.07	0.188	0.133
Cov 1	3.79	3.48	0.186	0.137
Cov 2	3.80	3.49	0.185	0.136
Expt.	3.79	3.49	0.182	0.138

Another property of the new model is that the number of unstable phonon branches is reduced while many other features of the calculated dispersion, already present in the old model, and which can be partly seen in the experiments too, are also contained in the new model. This fact demonstrates that the dispersion is governed essentially by the long-range Coulomb forces in the crystal. In particular, we still find that O_X^P has a very high frequency, which is in agreement with the experiments but quite in contrast to a calculation in a conventional metallic screening approach neglecting long-range Coulomb interactions.[19] The latter calculation predicts O_X^P to be soft. Typical longitudinal-optical–transverse-optical (LO-TO) splittings of the E_u modes are found in the calculation as well as in the experiments, and there is a large "ferroelectric" split (A_{2u} discontinuity) in both the calculations (dots in Figs. 1, 2, 4, and 5 at Γ) and the experimental dispersion; see, for example, Fig. 3, where new experimental results for selected phonon branches in La_2CuO_4 from Ref. 15 have been reproduced and from which a large A_{2u} discontinuity is obvious. In contrast to the notion in Fig. 3, we have chosen the upper LO mode to define the "ferroelectric" split because we extract from our calculations that in this mode and in the corresponding lower TO mode the anion and cation sublattices vibrate against each other generating a large dipole moment. Finally, the O_Z^z mode is found to be the highest Λ_1 mode at the Z point in the insulating phase. This fact and also the strong increase of the corresponding Δ_1 branch is now also confirmed by the experimental neutron results in the insulating phase (Fig. 3).

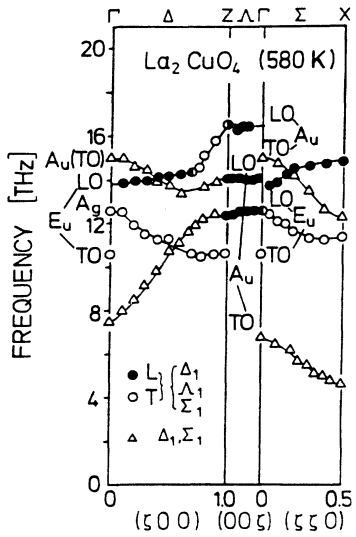

FIG. 3. Experimental phonon dispersion for selected phonon branches in the insulating phase of La_2CuO_4 in the main symmetry directions Δ, Λ, and Σ as reproduced from Ref. 15. The dispersion curves indicated by triangles should be labeled by the irreducible representations Δ_4, Σ_4 and not by Δ_1, Σ_1 in the notation of Ref. 15 and by Δ_3, Σ_3 in our notation.

Note in context with the calculations in the insulating phase of the HTSC's that we have introduced in Refs. 2–4 beyond the description by the purely ionic reference model an extension which likewise as in the case of the metal additionally allows for nonlocal, nonrigid screening effects of the charge-fluctuation type at the ions. To discriminate between the density response of a metal and that of an insulator the different long-wavelength behavior of the electronic polarizability Π is taken into account to set up the particular model for the insulating phase; see Refs. 2–4, 17 for more details. As far as the screening of the polar modes induced by such nonlocal charge response in the insulating phase is concerned, we find that the LO-TO splittings of the E_u modes are reduced in comparison to the ionic model. On the other hand, the "ferroelectric" splitting does not change at all and the highest Λ_1 branch, including O_Z^z, remains practically unchanged from the ionic model because of the two-dimensional electronic structure assumed. O_X^P, on the other hand, is decreased about 3 THz by the CF's leading to an agreement with the experiment.

Figure 4 collects our results for the phonon dispersion of the model with effective ionic charges in case we additionally allow for a simulation of covalence effects in the pair potentials by scaling the short-range part of the Cu-O_{xy} and La-O_{xy} potentials according to Eq. (5). With such a scaling procedure we can find by varying the R_0's a solution where the total interaction energy takes its minimum at structural parameters which are in excellent agreement with the observed structure;[20] see the model denoted as "Cov 1" in Table I. The width of the phonon spectrum in this model is again considerably reduced towards the experimental result and a good overall agreement throughout the Brillouin zone with the experimental dispersion is achieved; compare with Fig. 3. Moreover, nearly all unstable phonon branches disappear. One of the two remaining unstable phonon branches in the Σ direction corresponds at the X point to the tilt mode and the instability of this mode announces correctly the phase transition from the tetragonal to the low-temperature orthorhombic structure, which is shown by this calculation to be related to the ionic character of the forces. The other unstable branch along Σ corresponds at the X point to a (O_z, La) sliding motion perpendicular to the c axis. This displacement pattern leads to the conjecture that the scaling procedure additionally applied to the short-range part of the La-O_z potential will render this mode stable. This is indeed the case. The corresponding dispersion curves are shown in Fig. 5. Besides the now stable mode the dispersion is practically unchanged from the results displayed in Fig. 4. As a major effect only the low-frequency modes related to (O_z, La) sliding are improved. Moreover, the calculated structure parameters (Cov 2 in Table I) are in very good agreement with the experiments. In our subsequent calculations for the metallic phase we use the model Cov 1 as the reference model for the insulating phase.

Figures 6 and 7 show our results for the metallic phase of La_2CuO_4, including nonlocal screening effects of the CF type at the Cu and O_{xy} ions in the CuO plane. Physically this means that d-like and p-like localized electrons are not rigidly bound to their cores and thus allow for a nonlocal (nonrigid) contribution to the electronic-density response and to the EPI in the form of localized CF's at

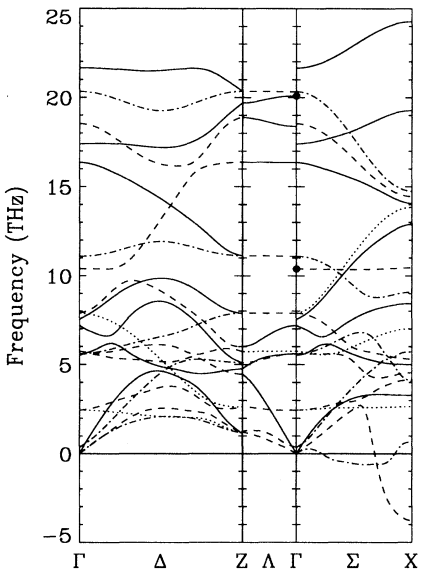

FIG. 4. Calculated phonon dispersion of the reference model Cov 1 for La_2CuO_4 using effective ionic charges and allowing for a scaling of the short-range part of the pair potentials Cu-O_{xy} and La-O_{xy}. The labeling of the curves is the same as in Fig. 2.

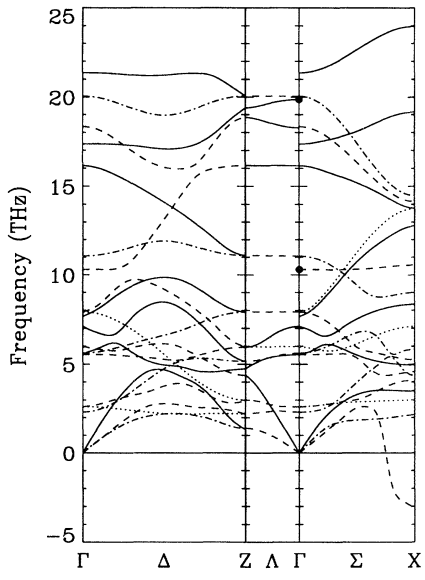

FIG. 5. Phonon dispersion of the reference model Cov 2 for La_2CuO_4 with effective ionic charges and scaling the short-range part of the pair potentials Cu-O_{xy}, La-O_{xy}, and La-O_z. The labeling of the curves is the same as in Fig. 2.

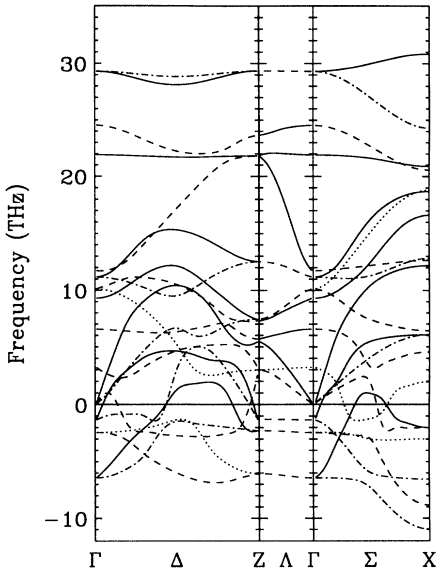

FIG. 6. Phonon dispersion of metallic La_2CuO_4 in the main symmetry directions Δ, Λ, and Σ taking charge fluctuations in the adiabatic approximation into account. As reference model the ionic model with nominal charges shown in Fig. 1 has been used. The labeling of the curves is the same as in Fig. 2.

these ions. In this way a strong nonlocal charge response can be induced in the CuO plane in particular for axial movements of the ions in the ionic layers of the HTSC's (like in O_Z^z) because of the reduced electronic screening along the c axis. At the same time a nonadiabatic description is essential for certain high-frequency modes

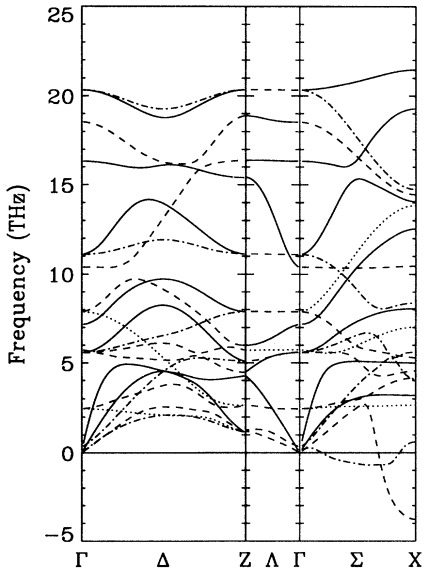

FIG. 7. Calculated phonon dispersion curves for metallic La_2CuO_4 along the Δ, Λ, and Σ directions including charge fluctuations in the adiabatic approximation. As reference model the model from Fig. 4 is used. The curve labeling is as in Fig. 2.

propagating along the c direction; see Sec. IV. This localized ionic picture for the metallic phase of the HTSC's is quite different from the charge response in conventional metals and superconductors where the (delocalized) homogeneous electron gas description for the electrons is a good starting point and correlated electron behavior is not so important in general. Figure 6 shows the results which are based on the ionic reference system with nominal charges (Fig. 1). The dispersion is almost unchanged from that in Ref. 3 where a simpler model for the electronic polarizability and different values for the B's and $\tilde{V}$'s have been used. In Fig. 7 the new model with effective charges and inclusion of covalence effects in the Cu-O_{xy} and La-O_{xy} potentials (Cov 1, Fig. 4) is taken as the reference system.

The calculations for the new model essentially reflect all the important features which can be seen in the experiments and which can be explained by the screening mechanism based on CF's and strong Coulomb correlation effects as discussed in detail in Ref. 3, using the old ionic model as a reference system. For example, the highest Δ_1 branch is decreased below Δ_4 in such a way that the experimentally observed situation is realized. At the same time the pronounced $\Delta_1/2$ minimum seen in the experiments appears and the LO-TO splitting is closed. The experimental and the calculated widths of the spectrum are now in very good agreement. As mentioned before, the O_X^P mode as the highest mode of the spectrum is at 21.46 THz, which has to be compared with 21.2 THz from the neutron study.[15]

Other prominent changes in the dispersion of the metallic phase as compared to the insulating phase are related to the screening effects brought about by the CF's for the polar modes. So all the LO-TO splittings are closed and a drastic renormalization of the spectrum occurs in context with the vanishing of the large A_{2u} discontinuity (ferroelectric split). Simultaneously this leads to a strong decrease of the second highest Δ_1 branch near the Z point as compared to the insulator and finally results in the appearance of a Λ_1 branch with a very steep dispersion, which is also found in the neutron-scattering results. At the same time the O_Z^z mode is strongly renormalized as compared to its value in the insulating material. The latter effect is due to the interplane charge transfer screening in the metallic phase which, on the other hand, is blocked in the insulating phase for a quasi-two-dimensional band structure; see Ref. 3 for details. From our calculations, displayed in Figs. 4 and 7, we conclude a renormalization for O_Z^z of $\Delta\nu=4.28$ THz. [The prediction of our former calculation (Refs. 2,3) was even higher, $\Delta\nu=6.13$ THz]. Such an anomalous renormalization which may be additionally enhanced in the nonadiabatic regime by mode coupling (see Sec. IV) has been confirmed quite recently by the experiments reporting a value of about 5 THz.[16]

IV. NONADIABATIC EPI AND PHONON-PLASMON MIXING

In the following we present the results of the new model (Cov 1) for the electron-phonon coupling in the adia-

batic and nonadiabatic regimes and investigate phonon-plasmon mixing along the c axis. Furthermore, consequences for the oxygen isotope effect due to the mode coupling are illustrated with an example. Different from the nonadiabatic case, in the adiabatic approximation the CF's do not spontaneously occur as plasmons but are driven by the ions in an adiabatic manner. In the nonadiabatic treatment the Cu d and O p CF's appear in the form of c-axis plasmons within the frequency range of the vibrational modes, mixing dynamically with the phonons of the same symmetry.

Our results for the phonon-induced site-potential changes δV_κ, according to Eq. (9), which measure directly the strength of the EPI in a certain mode, are given for O_Z^z in Table II. In agreement with the calculations performed using the old reference system[6] and with density-functional calculations reported in Ref. 5 we find also for the new model a large coupling strength in the adiabatic approximation, at least at the O_{xy} ions (Table II). From these investigations it becomes evident that the physical origin of the strong coupling is related to the weakly screened ionic forces present in the HTSC's especially in the c direction which are absent in the conventional metals and superconductors, respectively. Furthermore, it can be understood that the absolute values in Table II for δV_κ in the adiabatic approximation are smaller than the corresponding data in Ref. 6 because there is a reduction of the ionic charges and an increase of the distance between O_z and the CuO plane in the new model. Another source for the differences in δV_κ in the nonadiabatic regime is related to the fact that the reduced ionic charges together with the scaling of the short-range potentials lead to an exchange of the relative position of the free plasmon and the uncoupled phonon [dashed and dash-dotted lines in Fig. 8(a)] as compared to the situation found in Ref. 6. Simultaneously, the difference in frequency between the phononlike mode and the free plasmon is increased in comparison with the corresponding result in Ref. 6 and consequently the values for δV_κ are smaller in the new model. The reverse is true for the plasmonlike mode and thus the already very large coupling strength of this mode in the old model is even increased in the new one. Altogether, the important physics is the same in both calculations, namely, the strong enhancement of the coupling strength in the nonadiabatic regime which in detail depends on the relative position in the spectrum of the phononlike and plasmonlike modes with respect to the uncoupled plasmon.

Besides the position of the uncoupled phonon being determined to a large extent by the magnitude of the effective ionic charges, the relative position of the coupled modes is governed by the frequency of the uncoupled plasmon which is fixed by the electronic band structure in the axial direction. The latter will vary for different materials and with doping. These degrees of freedom may be utilized to obtain favorable conditions for pair binding via exchange of both elementary excitations by shifting the resonance frequencies of the phononlike and plasmonlike modes close together in order to optimize the attractive interaction between the electrons (holes) in the corresponding frequency range. In order to investigate these things more quantitatively it is necessary to improve the calculation of the electronic polarizability Π in our formalism installing for the calculation of Π, for example, the complete tight-binding parametrization of the local-density approximation band structure.[7] Such kinds of studies looking for the doping dependence of the phonon-induced site potentials and of the phonon-plasmon mixing are presently being performed. From the experimental fact that La_2CuO_4 is a HTSC with a relatively low T_c value it can be expected that the favorable resonance conditions mentioned above are not so well

TABLE II. Magnitudes of the phonon-induced site-potential changes δV_κ according to Eq. (9) for the O_Z^z mode. The first line of each entry gives δV_κ in units of meV and the second line displays the results for $(\delta V_\kappa)^2$ normalized by $\hbar/2M\omega(O_Z^z)$ in units of $(\text{eV/a.u.})^2$. M is the total mass in the unit cell. The data indicated by Ad correspond to the metallic phase of La_2CuO_4 treated in the adiabatic approximation. The last two entries collect the results for the phononlike (Ph) and plasmonlike mode (Pl) of the nonadiabatic calculation.

O_Z^z	Cu	O_{xy}
Ad	9.44	81.71
	0.31	23.12
Ph	188.57	78.07
	112.37	19.26
Pl	1938.10	1716.36
	24458.14	19181.73

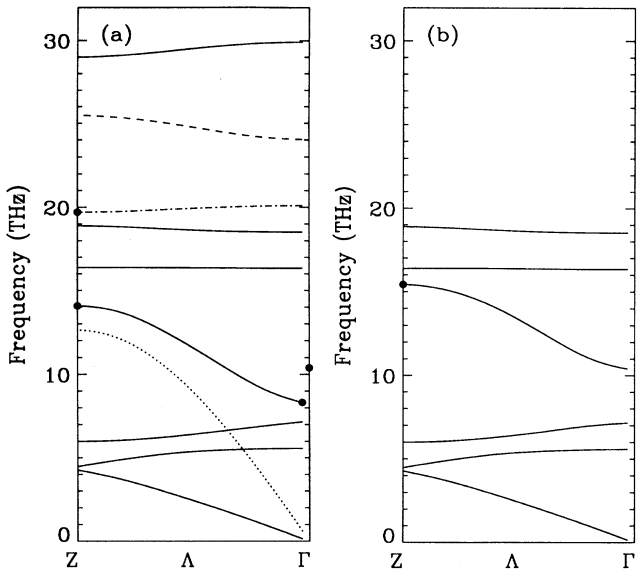

FIG. 8. (a) Calculated phonon (plasmon) dispersion in La_2CuO_4 along the $\Lambda\sim(0,0,1)$ direction. ——, Λ_1 symmetry branches of the coupled system; —·—·—·, uncoupled phonon; — — —, uncoupled plasmon; · · · · borderline for damping. (b) Λ_1 phonon branches in the adiabatic approximation. The reference system Cov 1 is used (Fig. 4).

fulfilled in this material.

In Fig. 8(a) we display our results for the phonon-plasmon mixing along the $\Lambda\sim(0,0,1)$ direction using the new reference model. For Π the same model as in Ref. 6 (model M_1) is used where the interlayer hopping parameters were chosen to give a maximal bandwidth in the c direction of about 50 meV at the Fermi level, in accordance with typical band structure results (Refs. 1,8). Comparing with the calculation in Ref. 6 the free plasmon and uncoupled phonon have interchanged their positions in the spectrum as discussed above and the phononlike branch at the Γ point (lower dot) has changed. The other features of the dispersion curves are similar to those in Ref. 6. The plasmon in Fig. 8(a) will couple along the Λ direction (mainly) to A_{2u}^{LO} (ferro) at Γ and to O_Z^z at the Z point. Comparing our result for the O_Z^z frequency in the insulating phase [upper dot at Z in Fig. 8(a)] with the result for O_Z^z in the adiabatic metal [dot in Fig. 8(b)] we extract the strong renormalization of $\Delta\nu=4.28$ THz already mentioned in Sec. III and related to an adiabatically phonon-driven interplane charge-transfer process in terms of CF's localized at the ions. This large decrease in frequency is further enhanced in the present model by the mode-coupling effect in the nonadiabatic calculation [lower dot at the Z point in Fig. 8(a), $\Delta\nu=5.63$ THz]. It should be remarked that this nonadiabatic contribution to the O_Z^z renormalization will depend in particular on the position of the free plasmon and thus on the realistic dispersion of the electronic band structure in the c direction. In any case, there will be a nonadiabatic contribution; the large value of 1.35 THz might be an intrinsic property of the present model. An implementation of the full tight-binding parametrization of the electronic band structure for the calculation of Π and an investigation of the nonadiabatic O_Z^z renormalization as a function of doping would be necessary to obtain a more quantitative understanding of this mode-coupling effect. Looking to the experimental situation for O_Z^z, an anomalous decrease in frequency of about 5 THz as predicted by our calculations has been communicated quite recently.[16]

In the adiabatic approximation, Fig. 8(b), there are six Λ_1 branches (see also Fig. 7), while in the nonadiabatic coupled-mode treatment as shown in Fig. 8(a) an additional plasmonlike branch appears. This extra branch is the highest branch in the spectrum. Note in this context that a plasma frequency of about 30 THz has been observed in the c-axis optical response in $YBa_2Cu_3O_7$.[21] Further experimental evidence for the existence of low-lying coupled phonon-plasmon modes in the HTSC's comes from the analysis of the $\mathbf{E}\|c$ infrared reflection spectra of $YBa_2Cu_3O_7$.[22] The phononlike branch starts at Γ with A_{2u}^{LO} (ferro) (lower dot) and terminates at Z with O_Z^z (lower dot at the Z point). Increasing the dispersion of the electron band structure in the c direction in our model means that we approach the adiabatic regime and the phononlike mode turns into its adiabatic shape, Fig. 8(b). At the same time, the ferroelectric split between A_{2u}^{LO} (ferro) and A_{2u}^{TO} (ferro) [upper dot in Fig. 8(a) at Γ] is closed from below and the plasmonlike mode is shifted to high frequencies.

A final remark is concerned with the oxygen isotope effect in the HTSC's. The strong mode coupling of the plasmon with oxygen-dominated phonons like O_Z^z leads to a reduction of the oxygen isotope effect in proportion to the plasmon character of these modes (provided they give a substantial contribution to the pairing as indicated by our calculations). We illustrate this matter by means of polar scattering in the diatomic case in the long-wavelength limit. Under the assumption that the Allen-Dynes strong-coupling equation can be applied for a determination of T_c, and if we assume a mass dependence through the frequency prefactor only, the isotope exponent α can be derived as

$$\alpha=\lambda^{-1}\sum_j \lambda_j\alpha_j\ ,\quad \lambda=\sum_j \lambda_j\ . \tag{10}$$

The λ_j are the mode-coupling strengths and the α_j are defined by

$$\alpha_j=-\frac{\partial \ln\omega_j}{\partial \ln M}\ . \tag{11}$$

In our case we have $j=\pm$ and $\omega_\pm$ are the frequencies of the coupled phonon-plasmon modes.

$$\omega_\pm^2=\tfrac{1}{2}(\omega_{\mathrm{LO}}^2+\omega_P^2)\pm\tfrac{1}{2}[(\omega_{\mathrm{LO}}^2+\omega_P^2)^2-4\omega_P^2\omega_{\mathrm{TO}}^2]^{1/2}\ . \tag{12}$$

Finally, we obtain

$$\alpha_+=\tfrac{1}{2}-\beta_\pm\ ,$$
$$\beta_\pm=\frac{\omega_p^2}{4\omega_\pm^2}\frac{(\pm2)(\omega_\pm^2-\omega_{\mathrm{TO}}^2)}{[(\omega_{\mathrm{LO}}^2+\omega_p^2)^2-4\omega_p^2\omega_{\mathrm{TO}}^2]^{1/2}}\ . \tag{13}$$

ω_{LO}, ω_{TO}, and ω_P are the frequencies of the LO and TO mode and the (uncoupled) plasmon, respectively.

In the adiabatic limit, where we can neglect phonon-plasmon coupling, we have $\omega_p\gg\omega_{\mathrm{LO}},\omega_{\mathrm{TO}}$. This leads to $\alpha_+\to0$, $\alpha_-\to0.5$ and the normal isotope exponent $\alpha=0.5$ is recovered from Eq. (10), if the coupling strength of the plasmon is neglected. On the other hand, in case we have resonance coupling ($\omega_p=\omega_{\mathrm{LO}}$), we obtain

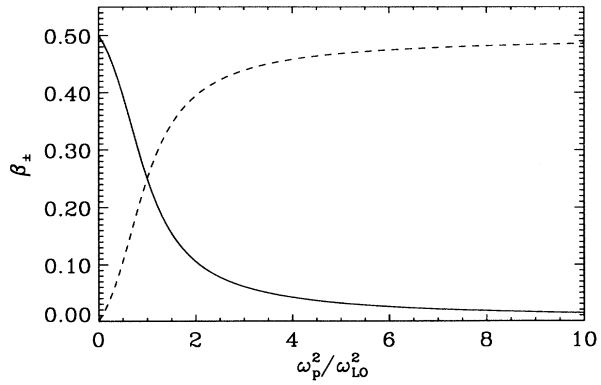

FIG. 9. $\beta_\pm$ from Eq. (13) as a function of $\omega_p^2/\omega_{\mathrm{LO}}^2$ for a fixed ratio of $\omega_{\mathrm{TO}}^2/\omega_{\mathrm{LO}}^2=0.75$. ω_{LO}, ω_{TO}, and ω_p are the frequencies of the LO mode, the TO mode, and the uncoupled plasmon. — — —, β_+; ——, β_-.

$\alpha_+ = \alpha_- = 0.25$ (see also Fig. 9), and thus the isotope exponent is reduced to $\alpha = 0.25$, independent from the individual mode-coupling strengths. Furthermore, the results displayed in Fig. 9 point towards the importance of the carrier concentration (via ω_p) in determining the size of the isotope exponent. The corresponding α for the phononlike mode (pieces of the curves in Fig. 9 with $\beta_\pm \leq 0.25$) has its minimum at the specific concentration related to the resonance condition and increases for deviations. The opposite is true for the plasmonlike mode (pieces of the curves in Fig. 9 with $\beta_\pm$ between 0.25 and 0.5).

V. SUMMARY

We have improved our microscopic model of rigid ions used for the description of the local part of the electronic-density response and the EPI in two steps. In the first step we have calculated effective ionic charges from a tight-binding analysis of the first-principles electronic band structure of La_2CuO_4. Subsequently, these charges are used instead of the nominal charges of our previous model for the calculation of the phonon dispersion. This calculation demonstrates that the overestimation of the width of the spectrum in the old model is considerably relaxed in the new model. In the second step we approximately include covalence effects in the pair potentials and find a further improvement of the phonon spectrum, which is now in good overall agreement throughout the Brillouin zone with the experimental dispersion for the insulating phase of La_2CuO_4. Moreover, all unstable phonon branches of the purely ionic model except the tilt mode have been shown to disappear.

In the case of the metallic phase, nonlocal screening effects in terms of charge fluctuations localized at the ions are taken into account in a parameter-free procedure. The calculated phonon dispersion explains the characteristic changes of the experimental results introduced by the insulator-metal transition. This gives additional support for the suitability of our density response description for the HTSC's. In particular, the large renormalization of the O_Z^z mode predicted by the calculations has been confirmed quite recently by the experiments. In the nonadiabatic regime, which is necessary for a description of the high-frequency phonons along the Λ direction, the mode-coupling effect with a low-lying plasmon additionally contributes to the renormalization of O_Z^z. The dynamical screening in the nonadiabatic calculation leads to an increase of the already large nonlocal electron-phonon coupling strength found in the adiabatic approximation. Especially for the plasmonlike mode very large changes of the phonon-induced site potentials are calculated. Furthermore, a low-energy plasmon and its mixing with certain phonons as seen in Ref. 6 is also present in the calculation given in this paper using the improved reference model. In this context it is important to realize that the existence of strong coupling low-energy plasmonlike and phononlike modes along the c axis as supported by our calculations may help to understand that part of the c-axis resistivity in the layered cuprate superconductors which displays a semiconductinglike temperature dependence as discussed in Ref. 23, where this part is related to a dynamical boson modulation of the interlayer hopping. The latter can be achieved by the low-energy plasmons and coupled c-axis phonons as intrinsic sources providing an activated hopping mechanism between the layers. Finally, we have outlined by means of a simple example that the oxygen isotope effect will depend on the carrier concentration in a characteristic way and can be severely reduced via phonon-plasmon mode coupling showing a minimum for the resonance case.

ACKNOWLEDGMENTS

We would like to thank Dr. L. Pintschovius for communicating his experimental results prior to publication and Dr. Q. Chen for his help in the numerical calculations. Further, we would like to express our thanks to Dr. R. Glasow and Dr. W. Zierau for the excellent management of the computer system in our department. Financial support by the Deutsche Forschungsgemeinschaft is gratefully acknowledged.

[1] W. E. Pickett, Rev. Mod. Phys. **61**, 433 (1989).
[2] C. Falter, M. Klenner, and W. Ludwig, Phys. Lett. A **165**, 260 (1992).
[3] C. Falter, M. Klenner, and W. Ludwig, Phys. Rev. B **47**, 5390 (1993).
[4] C. Falter, M. Klenner, and Q. Chen, Phys. Rev. B **48**, 16 690 (1993).
[5] H. Krakauer, W. E. Pickett, and R. E. Cohen, Phys. Rev. B **47**, 1002 (1993).
[6] C. Falter and M. Klenner, Phys. Rev. B **50**, 9426 (1994).
[7] M. J. De Weert, D. A. Papaconstantopoulos, and W. E. Pickett, Phys. Rev. B **39**, 4235 (1989).
[8] D. J. Singh, Physica C **212**, 228 (1993).
[9] R. G. Gordon and Y. S. Kim, J. Chem. Phys. **56**, 3122 (1972).
[10] R. E. Watson, Phys. Rev. **111**, 1108 (1958).
[11] F. Herman and S. Skillman, *Atomic Structure Calculations* (Prentice-Hall, Englewood Cliffs, NJ, 1963).
[12] J. P. Perdew and A. Zunger, Phys. Rev. B **23**, 5048 (1981).
[13] N. L. Allan and W. C. Mackrodt, Philos. Mag. B **69**, 871 (1994).
[14] C. Falter, Phys. Rep. **164**, Nos. 1 and 2 (1988).
[15] L. Pintschovius and W. Reichardt, in *Physical Properties of High Temperature Superconductors IV,* edited by D. M. Ginsberg (World Scientific, Singapore, 1994), pp. 295–374.
[16] L. Pintschovius (private communication).
[17] M. Klenner, C. Falter, and Q. Chen, Ann. Phys. (Leipzig) **3**, 225 (1994).
[18] M. Klenner, C. Falter, and Q. Chen, Ann. Phys. (Leipzig) **3**, 242 (1994).
[19] W. Weber, Phys. Rev. Lett. **58**, 1371 (1987).
[20] J. M. Longo and P. M. Raccah, J. Solid State Chem. **6**, 526 (1973).
[21] J. Schützmann, S. Tajima, S. Miyamoto, and S. Tanaka, Phys. Rev. Lett. **73**, 174 (1994).
[22] R. Gajic, E. K. H. Salje, Z. V. Popovic, and H. L. Dewing, J. Phys. Condens. Matter **4**, 9643 (1992).
[23] P. Nyhus, M. A. Karlow, S. L. Cooper, B. W. Veal, and A. P. Paulikas, Phys. Rev. B **50**, 13 898 (1994).